

CASE REPORT

Open Access



Epithelioid solitary fibrous tumors from CNS and soft tissues: an unusual morphologic variant

Lina Zhao^{1,2}, Jiajing Ma³, Jiakai Ren¹, Jingping Yuan¹, Huihua He¹, Yabing Huang¹ and Honglin Yan^{1*}

Abstract

Background Solitary fibrous tumors (SFTs) are distinctive soft tissue tumors characterized by rearrangements of *NAB2-STAT6* gene, which are associated with thin-walled, branching, “staghorn”-shaped vessels. SFTs are originally classified as a type of hemangiopericytoma (HPC). Classical SFTs are composed of spindle to ovoid cells arranged haphazardly or in fascicles. Rarely, SFTs exhibit unusual morphological variants such as fat formation, giant cells, dedifferentiation, or epithelioid variant. The epithelioid cell variant, which is composed almost entirely of epithelioid cells and arranged in solid or nest patterns, is extremely rare and frequently malignant.

Case presentation In this study, we reported three cases of epithelioid SFTs (ESFTs) located in extrathoracic sites (right lateral ventricle, right lumbar, left pelvis). All the subjects in this study were elderly, with a predominance of female patients, accounting for two out of the three cases, and only one case involved a male patient. The tumor cells were entirely composed of epithelioid cells and exhibited positive for CD34 and STAT-6 markers. Ultimately, the majority of cases (two out of three) were diagnosed as malignant SFTs.

Conclusion This study aims to enhance the awareness of ESFTs. In these cases, irrespective of the onset location, the arrangement patterns of tumor cells, such as papillary structures and the morphology of epithelial-like cells, conspicuously lack the hallmark histological characteristics of Solitary Fibrous Tumors (SFTs). Consequently, it requires differential diagnosis from a plethora of malignant neoplasms. Moreover, the elevated malignancy level of this cohort of cases poses substantial diagnostic challenges to pathologists, compounding the complexity of accurate interpretation.

Keywords Solitary fibrous tumors, Epithelioid cells, Papillary pattern

*Correspondence:

Honglin Yan
honglin@whu.edu.cn

¹Department of Pathology, Renmin Hospital of Wuhan University, Wuhan, Hubei 430060, China

²Department of Pathology, The Fifth Division Hospital of Xinjiang Production and Construction Corps, Xinjiang Uygur Autonomous Region, Bole 833400, China

³Department of Digestion and Rheumatology, The Fifth Division Hospital of Xinjiang Production and Construction Corps, Xinjiang Uygur Autonomous Region, Bole 833400, China



© The Author(s) 2024. **Open Access** This article is licensed under a Creative Commons Attribution-NonCommercial-NoDerivatives 4.0 International License, which permits any non-commercial use, sharing, distribution and reproduction in any medium or format, as long as you give appropriate credit to the original author(s) and the source, provide a link to the Creative Commons licence, and indicate if you modified the licensed material. You do not have permission under this licence to share adapted material derived from this article or parts of it. The images or other third party material in this article are included in the article's Creative Commons licence, unless indicated otherwise in a credit line to the material. If material is not included in the article's Creative Commons licence and your intended use is not permitted by statutory regulation or exceeds the permitted use, you will need to obtain permission directly from the copyright holder. To view a copy of this licence, visit <http://creativecommons.org/licenses/by-nc-nd/4.0/>.

Introduction

Solitary fibrous tumors (SFTs) are relatively rare mesenchymal tumors that were first described in 1931 by Klemperer and Rabin as pleural neoplasms [1]. The term “hemangiopericytoma” (HPC) was introduced in 1942 by Stout and Murray, attributed to the presence of hemangiopericytomatous vascular structures. The estimated incidence of SFTs is less than 2% of all soft tissue tumors, with approximately 0.2 cases per 100,000 individuals reported annually by Kayani et al. [2].

Initially, SFTs were only documented in the pleura and lungs until 1990, when they were noted to occur in various anatomical locations. They can originate from various soft tissues in the body, including the head and neck areas (including intracranial), pleural/mediastinal cavity chest, abdominopelvic region, and retroperitoneum. They typically present as painless, slow-growing masses with well-defined borders. The discovery of an intrachromosomal inversion at 12q13.3 in SFTs, which leads to the fusion of the NGFI-A binding protein 2 (NAB2) and *STAT6* genes, was a significant breakthrough [3, 4]. After that, SFTs were regarded as a distinct tumor entity with a well-defined molecular characteristic. In the 5th edition of the WHO Classification of Soft Tissue and Bone Tumors, SFTs are classified as fibroblastic neoplasms with intermediate behavior and rare metastasis.

Variants of SFTs, such as multinucleated giant cells, pseudopapillary, and epithelioid cytomorphologies, are uncommon. Epithelioid SFTs (ESFTs) are exceptionally rare, with few cases reported in the literature [5]. In this study, we reported three cases of ESFTs located in extrathoracic sites. Among them, one case was located in CNS (right lateral ventricle), the other two cases were located in soft tissues (right lumbar and left pelvis), presenting as medium to large epithelioid cells arranged in solid sheets and focal papillary patterns around vessels. These tumors were hypercellular and lacked the characteristic collagenized interstitium. Diagnostic clues can be derived from conventional SFTs features, mainly including the presence of curved vessels resembling HPC-like vessels. All tumor cells diffusely expressed STAT6 and CD34, while being negative for keratins, EMA, HMB45, SSTR-2, GFAP, CDK4, and MDM2.

Case presentation

Three cases of ESFTs were collected from Department of Pathology, Renmin Hospital of Wuhan University. Two senior pathologists independently reviewed the cases. Formalin-fixed paraffin-embedded (FFPE) tissue blocks were sectioned at a thickness of 4- μ m and stained with hematoxylin and eosin (H&E) using standard protocols.

Immunohistochemical analysis was performed on 4- μ m FFPE tissue sections using the following antibodies and conditions: STAT6 (ZSGB-BIO, clone: EP325),

CD34 (Dako, clone: QBEnd10), S-100 (Dako, clone: BC28), cytokeratin (CK or AE1/AE3, Dako, clone AE1/AE3), epithelial membrane antigen (EMA, Dako, clone 12E7), HMB45 (Dako, clone 6 F-H2), MelanA (Dako, clone: A103), Mum1 (Dako, clone: MUM1p), somatostatin receptor-2 (SSTR-2, ZSGB-BIO, clone: EP336), glial fibrillary acidic protein (GFAP, Dako, clone : 5.8 A), CDK4 (ZSGB-BIO, clone EP162), MDM2 (OriGene, clone: TA368038), progesterone receptor (PR, Roche, clone:1E2), thyroid transcription factor-1n(TTF-1, Dako, clone: 8G7G3), Ki67 (Dako, clone: MIB-1). The Envision Plus detection system (Dako) was used for all antibodies. Standard procedures and antigen retrieval protocols were followed. Appropriate positive and negative controls were included throughout.

Case 1 (located in CNS)

A 56-year-old woman was admitted to the hospital on June 16, 2021, presenting with dizziness and headache persisting for over four days. The medical history indicated that she had undergone resection of the right occipital space-occupying lesion in 2004, but the pathology diagnosis remained unknown. The recent episode of dizziness and headache did not involve nausea, vomiting, disturbance of consciousness, or cognitive impairment. Magnetic resonance imaging (MRI) findings suggested that a cystic-solid blood-rich space-occupying lesion was located in the right lateral ventricle, exerting pressure on the occipital lobe. Choroid plexus papilloma was considered as a possible diagnosis (Fig. 1A).

Intraoperatively, a cystic lesion with yellowish fluid was found in the right lateral ventricle, extending into the deep regions of the occipital lobe. Nodules with clear boundaries and a slightly firm texture were present at the posterior part of cystic region, partially adhered to the surrounding brain tissue. The tumor measured approximately 50 mm \times 60 mm \times 70 mm in size and displayed a gray-red appearance with soft consistency.

Gross examination: the surgical specimen consisted of multiple fragments, totaling approximately 80 mm \times 80 mm \times 25 mm, with a red-brown section and soft texture.

Microscopic findings showed that at low magnification, the tumor displayed clear boundaries with normal brain tissues and as mainly composed of distinct papillary structures (Fig. 1B). Two types of papillary structures were identified, including true papillary and pseudopapillary structures. True papillae consisted of single or multilayered medium-sized round or epithelial tumor cells surrounding thin-walled, slender, and curved vessels without obvious collagen (Fig. 1C). Pseudopapillary structures were formed by densely packed tumor cells around thick-walled vessels with evident hyalinization. Tumor cells were located centrifugally from the vascular

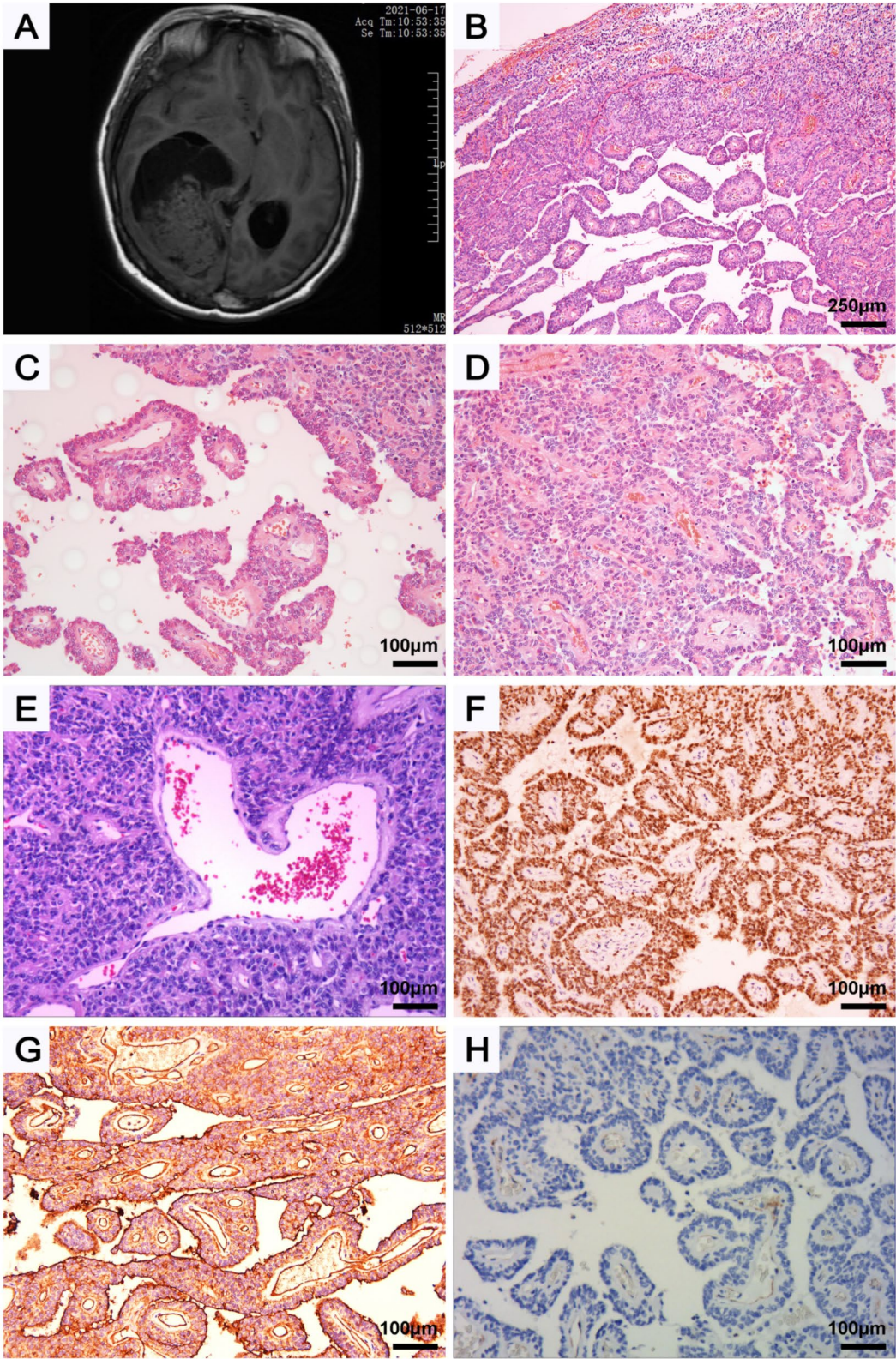


Fig. 1 (See legend on next page.)

(See figure on previous page.)

Fig. 1 Epithelioid solitary fibrous tumors of case 1. **A**, MRI showed a cystic- solid blood-rich space-occupying lesion in the right lateral ventricle, exerting pressure on the occipital lobe. **B**, At low magnification, clear boundaries were observed between the tumor and normal brain tissues, revealing almost entirely composed of distinct papillary structures. **C**, True papillae consisted of single or multilayered medium-sized round or epithelial tumor cells surrounding thin-walled, slender, and curved vessels without obvious collagen in their walls. **D**, Pseudopapillary structures were formed by densely packed tumor cells around thick-walled vessels with evident hyalinization. The tumor cells were located centrifugally from the vascular axis. **E**, Large, curved blood vessels can be seen within the interstitium. **F** to **H**, Immunohistochemistry showed diffuse nuclear expression of STAT6 (**F**) and cytoplasmic expression of CD34 (**G**), while staining was negative for SSTR-2 (**H**)

axis, with acellular areas near the vascular axis (Fig. 1D). The papillary spaces exhibited increased red blood cell extravasation, and large, curved blood vessels could be seen within the interstitium (Fig. 1E). At high magnification, a high cellular density and a disordered arrangement of uniform round and epithelioid cells with scant cytoplasm, oval nuclei, dense chromatin, and frequent mitotic Fig. (8/10 HPF) were noted. The tumor lacked classic SFTs features such as staghorn vessels and spindle cells, and was diagnosed as malignant solitary fibrous tumor (Grade 3) according to the diagnostic criteria in the 2021 World Health Organization Classification of Tumors of Central Nervous System (5th edition) [6].

By using immunohistochemistry, the tumor exhibited diffuse and intense nuclear staining for STAT6 (Fig. 1F), as well as diffuse staining for CD34 (Fig. 1G). The tumor was negative for EMA, SSTR-2 (Fig. 1H), GFAP, Olig-2, PR, S-100, Cytokeratin (AE1/AE3), and TTF-1. The Ki67 proliferation index was approximately 10%. It was diagnosed with malignant SFTs(CNS WHO G3).

Following tumor resection, the patient did not undergo any adjuvant radiotherapy or chemotherapy, as it was determined that the surgical margins were clear. The patient was followed up for six months post-surgery, during which time no significant complications were reported. However, after this period, the patient was lost to follow-up, preventing further assessment of long-term outcomes.

Case 2 (located in soft tissues)

An 85-year-old female patient was admitted to the hospital on March 24, 2023, due to A lumbar mass was identified six years prior and progressively enlarging over the past three years. Physical examination revealed a tough subcutaneous mass measuring 150 mm×100 mm on the right lower back, with well-defined margins, a smooth surface, acceptable mobility, and no tenderness. Clinically, a lipoma was suspected, and surgical excision was performed.

Macroscopic examination revealed a grayish mass measuring approximately 120 mm×95 mm×65 mm, with a partial capsule and a gray-red soft area. At low magnification, the tumor was located within the subcutaneous adipose tissue, possessing a well-defined boundary and incomplete capsules, along with local tongue-like infiltration into the adjacent adipose tissue. It consisted of large epithelioid cells and displayed various growth patterns,

such as solid sheet structures (Fig. 2A) and pseudopapillary arrangements (Fig. 2B). Similarly to Case 1, the papillary structure exhibited a pseudopapillary arrangement, which was characterized by multilayered tumor cells with weak adhesion around hyalinized blood vessels. The tumor cells possessed abundant cytoplasm that appeared eosinophilic or transparent in nature. Some tumor cells displayed eccentric nuclei akin to plasma cells (Fig. 2C). Notably, there were significant cellular atypia, multinucleated giant cells (Fig. 2D), brisk mitotic activity (Fig. 2E), limited collagen fibrosis, numerous thin-walled blood vessels with dilated congestion, focal nodular collagen formations, hemorrhage, necrosis, and ossification (Fig. 2F).

Through immunohistochemistry, the tumor showed diffuse nuclear strong staining for STAT6 (Fig. 2G) and diffuse staining for CD34 (Fig. 2H). SATB-2 was positive in the ossification region (Fig. 2I). In addition, the tumor cells exhibited focal positive for S-100-protein, with MUM1 positive scattered, but negative for EMA, SOX10, Melan A, CD138, Cytokeratin (AE1/AE3).The Ki67 proliferation index was approximately 20%~30%. The diagnosis was malignant SFTs.

After complete tumor resection, no adjuvant radiotherapy or chemotherapy was administered due to the patient's advanced age and associated comorbidities. During a 14-month follow-up period, the patient maintained good general health, with no evidence of recurrence or metastasis at the original site.

Case 3 (located in soft tissues)

An 85-year-old male patient was admitted to the hospital on September 24, 2021, due to a pelvic tumor that had been progressively growing for more than one year (Fig. 3A). Initial MRI and PET-CT scans on September 16, 2020, revealed a mass with uneven and increased metabolic activity in the soft tissue density of the left lateral wall of the pelvic cavity. The gross examination revealed a gray mass approximately 70 mm×50 mm×50 mm in size, with partial envelopment, focal hemorrhage, but no obvious signs of necrosis.

The tumor exhibited a well-defined boundary, a solid sheet or nodular pattern with abundant dilated or hyaline blood vessels within the tumor (Fig. 3A). It was composed of uniform medium to large-sized epithelial cells with transparent or acidophilic cytoplasm (Fig. 3B), which showed moderate atypia (Fig. 3C), and the mitotic

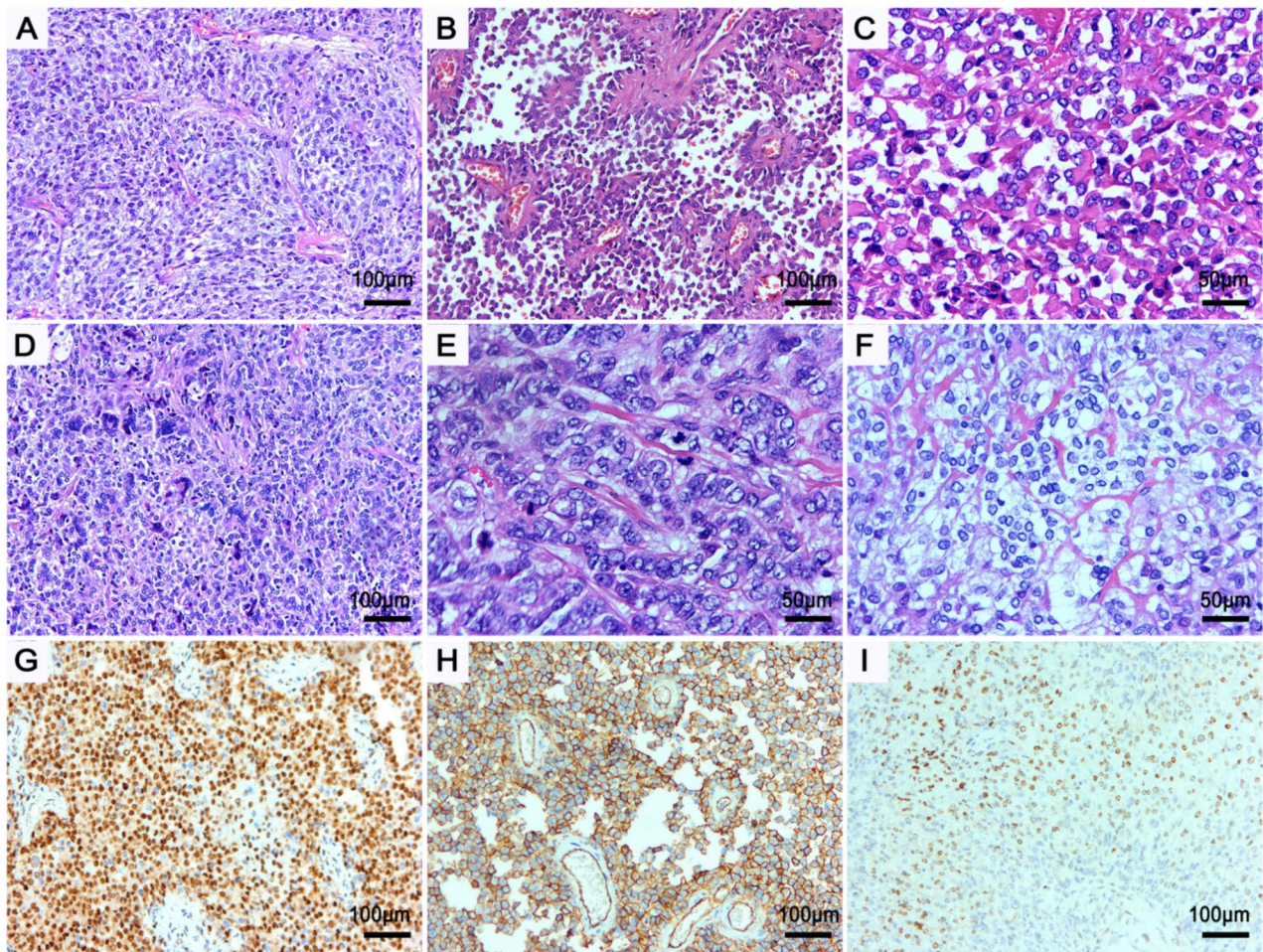


Fig. 2 Epithelioid solitary fibrous tumor of case 2. **A**, The tumor consisted of large epithelioid cells and displayed growth patterns with solid sheet structures. **B**, The tumor consisted of epithelioid cells and displayed growth patterns with papillary or pseudopapillary arrangements. **C**, Some tumor cells displayed eccentric nuclei akin to plasma cells. **D**, Significant cellular atypia was observed, even with the formation of multinucleated giant cell. **E**, Tumor cells showed brisk mitotic activity. **F**, Focal ossification can be observed. **G** to **I**, Immunohistochemistry showed diffuse nuclear expression of STAT6 (**G**) and cytoplasmic expression of CD34 (**H**), with SATB-2 positive in the ossification region (**I**)

count was 2 mitoses per 10 high-power fields with a diameter of 0.5 mm. Moreover, there was focal osseous matrix deposition (Fig. 3D). The tumor center exhibited features of stale hemorrhagic and collagenous nodules formation (Fig. 3E).

Immunohistochemical staining revealed diffuse and strong nuclear expression of STAT6 (Fig. 3F) as well as diffuse staining for CD34 (Fig. 3G) in the tumor cells, and SATB-2 was positive in the ossification region (Fig. 2H). While the tumor cells were negative for CDK4, MDM2, CD117, DOG1, S-100, HMB45, Cytokeratin (AE1/AE3), and EMA. The Ki67 proliferation index was approximately 5%. The final diagnosis was benign SFT. The risk stratification based on the three-variable and modified four-variable risk models was intermediate.

Following a 33-month postoperative follow-up period, during which the patient did not undergo radiotherapy or chemotherapy, recent CT scans and MRI examinations

revealed no signs of recurrence or metastasis. At present, the patient's overall condition remains satisfactory.

Discussion

Histological features

In 2003, Marchevsky et al. [7] characterized a mediastinal tumor that was predominantly comprised of epithelioid cells, and subsequently coined the term “epithelioid SFTs” to describe this rare entity [5]. Conventionally, SFTs have been recognized as spindle cell tumors characterized by a disorganized architecture and hemangiopericytoma-like vasculature. To date, less than 10 cases of this specific tumor type have been documented in the literature [5, 8–13]. Among the 11 recorded cases, including the present three cases (Table 1), patient ages ranged from 30 to 85 years, with a mean age of 64.9 years. The gender distribution was relatively balanced, with a slightly higher number of males than females (6:5), yielding a 1.2

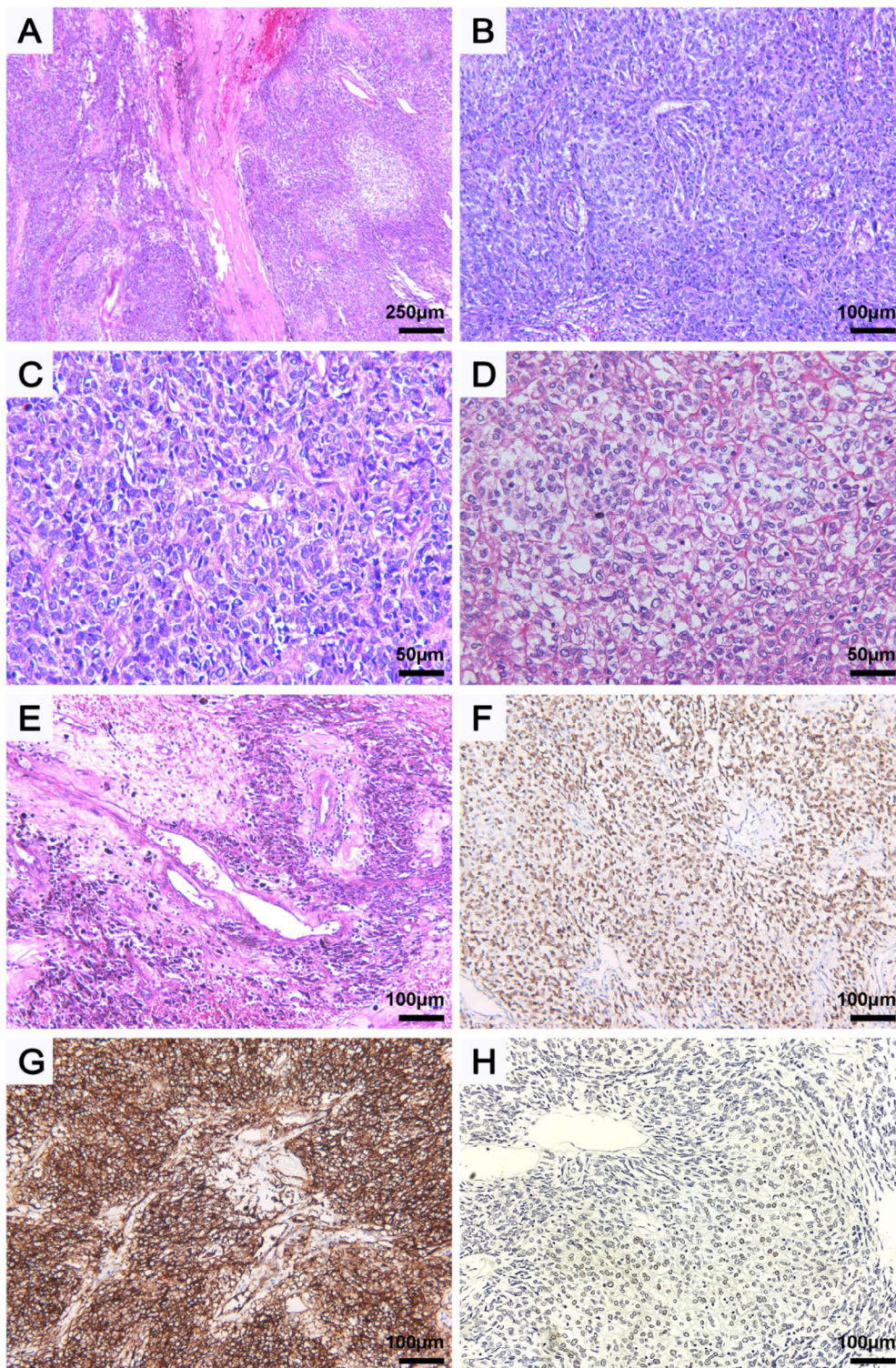


Fig. 3 Epithelioid solitary fibrous tumors of case 3. **A**, The tumor arranged in solid sheet or nodular pattern. **B**, The tumor was composed of uniform medium to large-sized epithelial cells, with transparent or acidophilic cytoplasm and abundant curved blood vessels in the center. **C**, Moderate atypia was observed. **D**, focal ossification and osseous matrix deposition. **E**, The tumor center exhibited features of stale hemorrhagic and collagenous nodules formation. **F to H**, Immunohistochemistry showed diffuse nuclear expression of STAT6 (**F**) and cytoplasmic expression of CD34 (**G**), with SATB-2 positive in the ossification region (**H**)

Table 1 Reported cases of epithelioid SFTs and their clinicopathological features

Authors and year	Age (years) at initial op/sex	Symptoms	Preoper course at initial op	Site	Size (cm)	Malignancy of epithelioid cells	STAT-6	Treatment	Outcomes	Follow-up duration (months)
Marchevsky et al. (2003)	74, M	Asymptomatic	NA	Posterior aspect of superior mediastinum	4.7	No	NA	Mass resection	NA	NA
Mourra et al. (2005)	67, M	Urinary problem	NA	Right ischioanal fossa	13.0	No	NA	Excision (complete)	ANED	6
Awasthi et al. (2006)	63, M	No tender Swelling	NA	Right neck	4.0	Yes	NA	Excision +	NA	NA
	57, M	Mass	15 years	Left ischioanal fossa	12.0	Yes	NA	RT Excision	NA	NA
Warraich et al. (2006)	71, M	Swelling and pain	Several weeks	Right orbit	NA	No	NA	NA	NA	NA
Martorell et al. (2007)	63, F	Mass, leg pain	3 years	Left thigh	10.0	Yes	NA	Excision + RT	ANED	6
Yan et al. (2008)	59, M	Unstable angina	NA	Pleura	9.7	Yes	NA	NA	NA	NA
Fu et al. (2012)	30, F	Headache and dizziness	7 months	Parietooccipital region	16.0	Yes	NA	Total excision	reexcision	85
Present cases	56, F	Headache and Dizziness	7 months	right lateral ventricle	8.0	Yes	+	Excision (complete)	Lost	Lost
	85, F	lumbar mass	3years	right lumbar	12.0	Yes	+	Excision (complete)	ANED	14
	85, M	pelvic tumor	1year	left pelvis	7.	No	+	Excision (complete)	ANED	33

NA=not available; ANED=alive, no evidence of disease; RT=radiation therapy

:1 ratio. These lesions were located in various anatomical locations, such as mediastinum [5], orbit [10], ischioanal fossa, neck [8], thigh [9], pleura [12], and central nervous system [13], with the majority being found in extrapleural locations. The size of these tumors at the time of initial resection ranged from 4.0 cm to 13.0 cm.

Microscopically, the majority of cases (6 cases) exhibited a biphasic pattern, consisting of both spindled and epithelioid cell regions, while 3 cases in this study were purely composed of epithelioid cells. The epithelioid cells were arranged in solid sheets, cords, nests, and pseudoglandular or cleft patterns, exhibiting both epithelioid and round cell morphology. This was manifested by marked hypercellularity, frequent mitotic activity (ranging from 5/10 HPF to abundant mitotic figures), significant pleomorphism, and nuclear atypia. All the cases we reported were purely epithelioid. In addition to solid sheets and nests, papillary and pseudopapillary structures were first described in the present cases. All cases exhibited malignant or atypia characteristics, such as large tumor size, hypercellularity, significant pleomorphism, and brisk mitoses, suggesting that these epithelioid regions may indicate areas of malignant transformation.

Immunohistochemical features

The commonly observed positive immunohistochemical markers in SFTs are STAT6, CD34, BCL2, and CD99. The combination of this panel is highly sensitive and specific, typically showing diffuse and strong expression in almost all cases. Due to the presence of *NAB2-STAT6* gene fusion in SFTs, immunohistochemical staining STAT6 serves as a useful surrogate marker with excellent sensitivity and specificity. It is expressed in both benign and malignant cases [3, 14, 15]. The other three markers are less useful when used alone, as they are also expressed in other neoplasms resembling SFTs [16], so although they exhibit sensitivity, they lack specificity [17]. CD34 is also valuable for SFTs, being expressed in 81–95% of these tumors, but its expression may decrease or become negative in malignant or dedifferentiated tumors [18]. It is important to note that STAT6 can also be expressed in other soft tissue neoplasms, such as dedifferentiated liposarcoma (DDL) or well-differentiated liposarcoma (WDL), as well as in desmoid fibromatosis, undifferentiated pleomorphic sarcoma, and synovial sarcoma (SS) [19, 20].

Some instances of ESFTs may exhibit multifocal cytokeratins positivity. But EMA was negative in all reported cases of ESFTs [5, 8]. Furthermore, there was no expression of h-caldesmon, Desmin, and S100. Malignant cases tend to display TP53 positivity [21]. In this study, although the morphology displayed epithelioid features in all cases, none exhibited positive for cytokeratins or EMA.

Molecular features

The fusion of *NAB2* and *STAT6* genes is present in the majority of SFTs and can be identified using next-generation sequencing (NGS) and reverse-transcription polymerase chain reaction (RT-PCR) techniques. *NAB2* and *STAT6* genes are located very close to each other on chromosome 12, making it difficult to detect these fusions by FISH technique [22]. While Barthelme et al. [23] detected the fusion of these two genes in 92% of cases by using RT-PCR. In SFTs, the fusion of *NAB2* and *STAT6* genes exhibits approximately 12 distinct types of gene fusions, with three variants being most prevalent, accounting for 75% of all types. Tumors harboring the *NAB2ex4-STAT6ex2/3* fusion variant, predominantly situated within the thoracic cavity, displayed classic fibrous SFTs morphology, and were associated with an older patient demographic, larger tumor dimensions, a reduced mitotic index, and lower recurrence rates. In contrast, the truncation mutation of *NAB2ex6-STAT6ex16* and *NAB2ex6-STAT6ex17* fusion variants were predominantly identified in younger patients, characterized by smaller tumor size, elevated mitotic activity, a cellular SFTs or typical HPC morphology, and increased recurrence rates [23]. In this study, Case 1 presented an intracranial Solitary Fibrous Tumors (SFTs) characterized by papillary structures. According to the literature, among nine documented cases of intracranial SFTs with papillary architecture, 57% underwent *NAB2-STAT6* fusion gene analysis, and all (100%) exhibited the *NAB2ex6-STAT6ex17* fusion gene, representing a truncating mutation in the *STAT-6* gene. Consequently, this histological variant of SFTs frequently manifests malignant characteristics and exhibits a higher propensity for recurrence [24]. Although distinctions in gene fusion variants are observed between pleural and extrapleural locations, Yamada et al. and Park et al. did not identify a direct correlation between these fusion variants and malignancy. Nevertheless, the association between gene fusion variants and tumor location has the potential to influence the biological behavior of SFTs [21, 25]. Promoter mutations in the *TERT* gene have been implicated in malignant SFTs in two studies [21, 26]. *TP53* mutations have been detected in approximately 41% of malignant SFTs [20]. Dedifferentiated SFTs also characteristically exhibit *TP53* mutations [24, 27].

Differentiated diagnosis

Soft tissue tumors displaying epithelioid characteristics, such as epithelioid sarcoma and epithelioid angiosarcoma, need to be considered in the differential diagnosis of SFTs [27]. Epithelioid sarcoma is commonly detected in the soft tissues of the limbs, presenting an infiltrative growth pattern and consisting of both epithelioid and spindle cells. The epithelioid cells are located in the center and are polygonal or oval in shape, with abundant cytoplasm, eosinophilic plasma, and small nucleoli. The spindle cells are often located around the periphery and may show haloing. The tumor cells are typically positive for AE1/AE3, EMA, CK7, CK19, and CD34, with more than 95% of cases showing a loss of SMARCB1 (INI1) expression [28]. *STAT6* is typically negative in epithelioid sarcoma, which is helpful for differential diagnosis. Epithelioid angiosarcoma is a rare malignant tumor that originates from endothelial cells, mainly occurs in the thighs and buttocks of elderly patients, and is characterized by clusters and sheets of acidophilic, oval-shaped epithelium-like cells, along with numerous blood vessels forming fissures and networks within the tumor. Immunohistochemically, it shows vascular-derived markers (CD31, CD34, Factor VIII, Fli-1, and D2-40) positivity. Though both of them are positive for CD34, *STAT6* is typically negative in epithelioid angiosarcoma, which is helpful for differential diagnosis.

Among the cases in this study, one occurred in the cranial cavity and was arranged in a papillary pattern, thus it was necessary to differentiate it from similar intracranial lesions, such as primary papillary tumors and metastatic papillary carcinoma of the dura mater externa. Papillary meningiomas typically occur in the meninges, and are characterized microscopically by an eccentric stratified papillary structure. They are positive for EMA and SSTR2, but negative for CD34 and *STAT6*, which can be used for differential diagnosis. Papillary ependymomas commonly occur in the ventricles and spinal cord, characterized by cuboidal cells surrounding the vessels. These tumors are positive for S-100 protein and exhibit GFAP expression in the tumor cells near the vessels. EMA in tumor cells is observed to exhibit perinuclear punctate positivity or a cytoplasmic ring-like structure. But CD34 and *STAT6* are negative in tumor cells, which can be utilized for differential diagnosis. Choroid plexus papillary tumors originate from the cells of the choroid plexus and are commonly observed in the ventricles of the brain, featuring single-layered columnar epithelial cells surrounding the vessels to form a papillary structure, with the nuclei located at the base. Immunohistochemical markers of choroid plexus papillary tumors include CKpan, S-100, and TTF1. But negative for CD34 and *STAT6*, which can be utilized for differential diagnosis. Metastatic papillary thyroid carcinomas are characterized by

papillary structures formed by columnar epithelial cells around blood vessels. Nuclear features include a honeycomb pattern, nuclear grooves, nuclear overlap, and nuclear pseudocysts. Immunohistochemical markers like CK19 and BRAFV600E in metastatic papillary thyroid carcinomas are not expressed in papillary SFT. Diffuse nuclear positivity for STAT6 in SFT but negativity in papillary thyroid carcinomas can be utilized for differential diagnosis.

Treatment and prognosis

Various clinical and histomorphological characteristics have been identified as potential indicators of malignancy, while SFTs occurring in CNS or soft tissues have different stratification criteria. According to the newly diagnostic criteria in the 2021 World Health Organization Classification of Tumors of Central Nervous System (5th edition) [6], the pathological grade of SFTs is based on two key indicators: the nuclear mitotic count at a threshold of 5/10 high-powered fields (HPF), and the presence or absence of necrosis. More precisely, the grading designations are as follows: Grade 1 SFTs exhibit a nuclear mitotic rate < 5/10 HPF; Grade 2 SFTs present with a nuclear mitotic rate \geq 5/10 HPF yet devoid of necrosis; and Grade 3 SFTs are characterized by a nuclear mitotic rate \geq 5/10 HPF and conjunction with necrotic tissue. However, in soft tissues, malignant SFTs are usually hypercellular lesions, showing increased mitoses (>4 mitoses per 10 HPF), variable cytological atypia, tumour necrosis, and/or infiltrative margins, among which mitoses seem to be most prognostic [29]. A set of risk calculators proposed by the French Sarcoma Group (FSG), being the most widely used model for metastatic risk, incorporates mitotic count (\geq 2 mitoses/mm²), patient age (\geq 55 years), and tumour size stratified by 5 cm tiers to classify tumours into low, intermediate, and high risk groups [30]. Subsequently, a refinement includes necrosis as a fourth variable. Recurrence and metastasis events are more prevalent in malignant SFTs [29]. A poor prognosis is associated with tumors located at extrathoracic sites. Tumors in the meninges, pelvis, retroperitoneum, and mediastinum pose a higher risk of recurrence [31]. All the cases in this study were located at extrathoracic sites, presenting cellularity, marked nuclear pleomorphism, and brisk mitotic activity. Thus, most of the cases corresponded to malignant SFTs and indicated a poor prognosis. All patients underwent surgical resection as the sole treatment approach, without any additional adjuvant radiotherapy or chemotherapy. During the present follow-up period, except for case one who was lost to follow-up, the other two patients maintained good general health and exhibited no signs of disease recurrence or metastasis. The presence of distant metastases served

as a poor prognostic indicator, with 75% of patients succumbing to their disease [32].

The main treatment approach for SFTs is wide surgical excision, with adjuvant radiotherapy and chemotherapy not being necessary. However, some studies suggest that adjunctive radiotherapy may enhance local tumor control. For meningeal tumors, surgical intervention alone is adequate for the SFTs of WHO grade 1, while tumors with WHO grades 2 and 3 may benefit from additional radiotherapy. Given the rarity of these tumors and the paucity of randomized controlled trials, there is no global consensus regarding their treatment. A multidisciplinary team approach is recommended for the management of these tumors.

Acknowledgements

Not applicable.

Author contributions

LZ contributed to the writing of the manuscript text. JR, JY, HH and YH acquired data. HY supervised the writing and revision of the manuscript. All authors contributed to the article and approved the submitted version.

Funding

This work was supported by grants from Natural Science Foundation of Hubei Province (2021CFB383) and the Science and Technology Plan Project of Shuanghe City, the Fifth Division of Xinjiang Production and Construction Corps (2024YL04).

Data availability

No datasets were generated or analysed during the current study.

Declarations

Ethical approval

Written informed consent was obtained from the patients/participants for the publication of this case study.

Competing interests

The authors declare no competing interests.

Received: 16 July 2024 / Accepted: 16 October 2024

Published online: 25 October 2024

References

1. Klemperer P, Coleman BR. Primary neoplasms of the pleura. A report of five cases. *Am J Ind Med.* 1992;22:1–31.
2. Kayani B, et al. A review of the Surgical Management of Extrathoracic Solitary Fibrous tumors. *Am J Clin Oncol.* 2018;41:687–94.
3. Yoshida A, et al. STAT6 immunohistochemistry is helpful in the diagnosis of solitary fibrous tumors. *Am J Surg Pathol.* 2014;38:552–9.
4. Chmielecki J, et al. Whole-exome sequencing identifies a recurrent NAB2-STAT6 fusion in solitary fibrous tumors. *Nat Genet.* 2013;45:131–2.
5. Marchevsky AM, Varshney D, Fuller C. Mediastinal epithelioid solitary fibrous tumor. *Arch Pathol Lab Med.* 2003;127:e212–215.
6. Louis DN, Perry A, Wesseling P, et al. The 2021 WHO classification of tumors of the Central Nervous System: a summary. *Neuro Oncol.* 2021;23(8):1231–51.
7. Gengler C, Guillou L. Solitary fibrous tumour and haemangiopericytoma: evolution of a concept. *Histopathology.* 2006;48:63–74.
8. Awasthi R, et al. Biphasic solitary fibrous tumour: a report of two cases with epithelioid features. *Virchows Archiv: Int J Pathol.* 2006;448:306–10.
9. Martorell M, et al. Solitary fibrous tumor of the thigh with epithelioid features: a case report. *Diagn Pathol.* 2007;2:19.

10. Mourra N, Lewin M, Sautet A, Parc R, Flejou JF. Epithelioid solitary fibrous tumor in the ischioanal fossa. *Virchows Archiv: Int J Pathol*. 2005;446:674–6.
11. Warraich I, Dunn DM, Oliver JW. Solitary fibrous tumor of the orbit with epithelioid features. *Arch Pathol Lab Med*. 2006;130:1039–41.
12. Yan B, Raju GC, Salto-Tellez M. Epithelioid, cytokeratin expressing malignant solitary fibrous tumour of the pleura. *Pathology*. 2008;40:98–9.
13. Fu J, et al. Epithelioid solitary fibrous tumor of the central nervous system. *Clin Neurol Neurosurg*. 2012;114:72–6.
14. Doyle LA, Vivero M, Fletcher CD, Mertens F, Hornick JL. Nuclear expression of STAT6 distinguishes solitary fibrous tumor from histologic mimics. *Mod Pathology: Official J United States Can Acad Pathol Inc*. 2014;27:390–5.
15. Schweizer L, et al. Meningeal hemangiopericytoma and solitary fibrous tumors carry the NAB2-STAT6 fusion and can be diagnosed by nuclear expression of STAT6 protein. *Acta Neuropathol*. 2013;125:651–8.
16. Vivero M, Doyle LA, Fletcher CD, Mertens F, Hornick JL. GRIA2 is a novel diagnostic marker for solitary fibrous tumour identified through gene expression profiling. *Histopathology*. 2014;65:71–80.
17. Miettinen M. Immunohistochemistry of soft tissue tumours - review with emphasis on 10 markers. *Histopathology*. 2014;64:101–18.
18. Han Y, et al. Immunohistochemical detection of STAT6, CD34, CD99 and BCL-2 for diagnosing solitary fibrous tumors/hemangiopericytomas. *Int J Clin Exp Pathol*. 2015;8:13166–75.
19. Doyle LA, Tao D, Mariño-Enríquez A. STAT6 is amplified in a subset of dedifferentiated liposarcoma. *Mod Pathology: Official J United States Can Acad Pathol Inc*. 2014;27:1231–7.
20. Demicco EG, et al. Extensive survey of STAT6 expression in a large series of mesenchymal tumors. *Am J Clin Pathol*. 2015;143:672–82.
21. Park HK, et al. Molecular changes in solitary fibrous tumor progression. *J Mol Med*. 2019;97:1413–25.
22. Mohajeri A, et al. Comprehensive genetic analysis identifies a pathognomonic NAB2/STAT6 fusion gene, nonrandom secondary genomic imbalances, and a characteristic gene expression profile in solitary fibrous tumor. *Genes Chromosomes Cancer*. 2013;52:873–86.
23. Barthelmeß S, et al. Solitary fibrous tumors/hemangiopericytomas with different variants of the NAB2-STAT6 gene fusion are characterized by specific histomorphology and distinct clinicopathological features. *Am J Pathol*. 2014;184:1209–18.
24. Yao ZG et al. Papillary Solitary Fibrous Tumor/Hemangiopericytoma: an uncommon morphological form with NAB2-STAT6 Gene Fusion. *J Neuro-pathol Exp Neurol* (2019).
25. Yamada Y et al. Clinicopathological review of solitary fibrous tumors: dedifferentiation is a major cause of patient death. 475, 467–77 (2019).
26. Bianchi G et al. Histological and molecular features of solitary fibrous tumor of the extremities: clinical correlation. 476, 445–54 (2020).
27. Machado I, et al. Controversial issues in soft tissue solitary fibrous tumors: a pathological and molecular review. *Pathol Int*. 2020;70:129–39.
28. Lyon F, WHO Classification of Tumours Editorial Board. Soft tissue and Bone Tumours. *WHO Classif Tumours*. 2020;3:330–2.
29. Fletcher CDM, et al. World Health Organization classification of tumours. Pathology and genetics of tumours of soft tissue and bone [M]. Lyon: IARC; 2013. pp. 10–238.
30. Salas S, et al. Prediction of local and metastatic recurrence in solitary fibrous tumor: construction of a risk calculator in a multicenter cohort from the French Sarcoma Group (FSG) database. *Annals Oncology: Official J Eur Soc Med Oncol*. 2017;28:1979–87.
31. Cranshaw IM, et al. Clinical outcomes of extra-thoracic solitary fibrous tumours. *Eur J Surg Oncology: J Eur Soc Surg Oncol Br Association Surg Oncol*. 2009;35:994–8.
32. Gold JS, et al. Clinicopathologic correlates of solitary fibrous tumors. *Cancer*. 2002;94:1057–68.

Publisher's note

Springer Nature remains neutral with regard to jurisdictional claims in published maps and institutional affiliations.